

A novel pulsed Doppler radar seeker modeling method used for closed loop trajectory simulation

Liandong Wang¹, Huanyao Dai^{1a}, and Hui Yang²

¹ State Key Laboratory of Complex Electromagnetic Environmental Effects on Electronics and Information System, Luoyang, 471003, China

² College of Computer, National University of Defense Technology, Changsha, 410073, China

a) leoneast@163.com

Abstract: This paper is dedicated to the coherent video modeling of pulsed Doppler radar seeker (PDRS) for the six degree of freedom (6-DOF) closed loop trajectory simulation, which provides an efficient tool to the design and evaluation of surface-to-air missile (SAM). The topics covered are wave-forms consideration, radar antenna modeling, target scattering characteristics, receiver processing, signal processor design and filter mechanism in data processing. The augmented proportional navigation law is used to generate the acceleration demands, while the bank-to-turn control command to obtain the fin-angle demand and the 6-DOF missile motion solution can then be accomplished by using SAM's aerodynamic characteristics. A typical air defense warfare scenario is designed to validate coherent video modeling as well as the 6-DOF closed loop trajectory simulation. The electronic countermeasures are also taken into account. Results show that VGPO has no direct effect on the angle tracking loop, just through guidance filter to affects the angular speed estimation astringency. It achieves only 2 towing cycle within a relatively short time of terminal guidance. The conclusion was consistent with the anechoic chamber measurements results, which proved that PDRS coherent video model is accurate for 6-DOF trajectory simulation. The paper provided an effective and practical solution for parameters designing and performance evaluation of tactical cruise missile.

Keywords: coherent video modeling, pulsed doppler, radar seeker, trajectory simulation, closed loop

Classification: Microwave and millimeter wave devices, circuits, and systems

References

- [1] J. Muller and J. Plorin: Proc. of the Society of Photo-Optical Instrumentation Engineers (Spie) (2001) 65.
- [2] H. Y. Dai and X. S. Wang: IEEE Trans. Antennas Propag. **60** (2012) 1653. DOI:10.1109/TAP.2011.2180321

- [3] H. F. Li and M. Zhao: 2010 International Conference on Information, Electronic and Computer Science (2010) 2010.
- [4] A. Farooq and D. J. N. Limebeer: *J. Guid. Control Dyn.* **31** (2008) 1076. DOI:10.2514/1.31441
- [5] Z. S. Jia and X. C. Si: 2009 IEEE International Conference on Intelligent Computing and Intelligent Systems (2009) 418. DOI:10.1109/ICICISYS.2009.5358141
- [6] J. B. Zou, K. Gao and E. Y. Zhang: *Przeglad Elektrotechniczny* **88** [3] (2012) 18.
- [7] P. Vora, P. K. Tiwari and R. N. Bhattacharjee: *Def. Sci. J.* **55** [3] (2005) 337.
- [8] C. Inaebnit, M. A. John and U. Aulenbacher: *Proc. of the Society of Photo-Optical Instrumentation Engineers* (2003) 235.

1 Introduction

Conventional functional modeling of PDRS, which is widely used in 6-DOF trajectory simulation due to its simpleness and convenience, can't reflect the process of electromagnetic wave propagation and scattering, as well as the coherent processing in receiver and consecutive digital signal processor, thus it is inefficient in accurate 6-DOF trajectory simulation, especially in the case of electronic countermeasures (ECM) [1, 2, 3, 4]. While, coherent video modeling completely describe the process of wave transmission, propagation, back scattering, antenna receiving, receiver processing, digital signal processing and maybe following data processing [5, 6]. It offers a comprehensive way to help design parameters and evaluate SAM's performance. The coherent video modeling due to its simulation precision leads to a relative high computation burden and a long development cycle, and, consequently, has interested few developers in the field of 6-DOF trajectory simulation, in which attention has often paid to missile aerodynamic characteristics, guidance law and control command. However, to perform an accurate closed loop trajectory simulation, one must get the coherent video model of PDRS finished somehow. This paper is organized as follows. Firstly, a brief description of the role of PDRS as a crucial angle sensitive device in SAM's guidance and control loop is discussed. Then various aspects of PDRS coherent video modeling are discussed. The topics covered are waveforms consideration, radar antenna modeling, target scattering characteristics, receiver processing, signal processor design and filter mechanism in data processing. A 6-DOF closed loop trajectory simulator is designed, and some key factors including guidance law and control command are taken into account. A typical air defense warfare scenario is planned to validate coherent video modeling as well as the 6-DOF closed loop trajectory simulation. Then the simulation and flight test results are discussed.

2 Coherent video modeling

2.1 PDRS configurations

There are several different implementations of PD radars depending on whether low-, medium-, or high-PRF waveforms are utilized. A basic decision that must be made in PDRS design is the selection of the PRF. It is known that PD radars can be categorized as low, medium and high PRF, according to whether Doppler (low PRF), range (high PRF), or both of them are ambiguous (medium PRF).

The choice among the various waveforms in PDRS mainly depends on SAM's application. Line-of-sight angles and their rates are necessary to obtain acceleration demands, while slant range and range rate measurements are somewhat unimportant, though they may be needed in target tracking loop and other advanced guidance law (as the optimal guidance law). As long as the angle tracking loop works, PDRS can sustain the basic homing guidance, whether the range or range rate information are correctly measured.

An example in [3] illustrates the problem of employing a low-PRF Doppler radar design for small aperture high-speed missile-borne radar seeker due to excessive spreading of main lobe ground clutter along the PRF lines, which blocks a large portion of the velocity region associated with the target. While, the medium-PRF for missile applications can provide slow-moving target rejection, all-target-aspect coverage and relative accurate range information. However, the range and Doppler ambiguities of a medium-PRF design cause the returns from short-range sidelobe clutter to fold into the same Doppler regions occupied by target returns, which dramatically increase the design complexity to resolve ambiguities. A high-PRF waveform provides a clutter-free target detection region that generally facilitates detection of closing targets, which is of great importance in surface-to-air operation. HPRF designs require complicated methods for resolving ambiguities of range, however, this is not necessary for SAM's tracking loop, as only one Doppler filter may be needed for tracking once the target is acquired. One can use quasi-continuous wave processing at the absence of range/range rate measurements to select targets that have particular radial velocities in heavy ground or sea clutter.

As discussed above, a HPRF waveform is utilized, and then the PDRS configurations are accomplished on the viewpoint of coherent video modeling, as depicted in Fig. 1. Some key parts in PDRS are discussed briefly as followed.

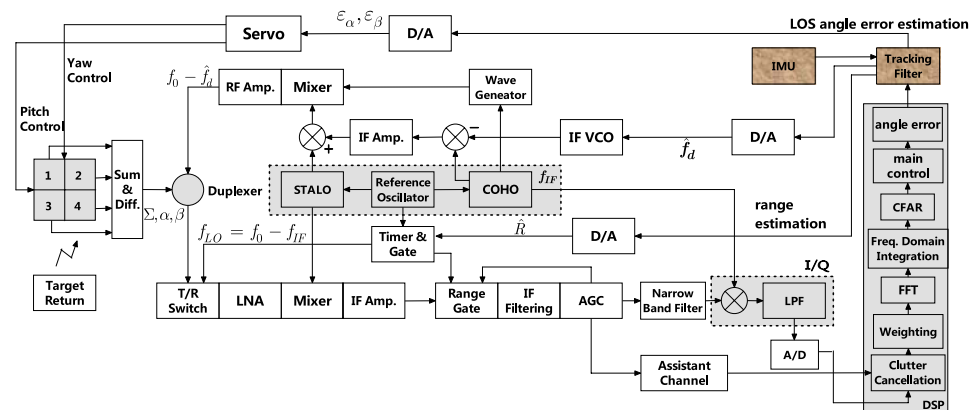


Fig. 1. Pulsed Doppler radar seeker configurations.

2.2 Antenna modeling

Antenna model is fundamental to PDRS simulation. A simplified antenna pattern of the single beam is established by using Sinc function, written as Eq. (1).

$$F(\theta) = G_0 \cdot \left| \frac{\sin(2\pi\theta/\theta_0)}{2\pi\theta/\theta_0} \right|, \quad \theta \leq \theta_0/2 \quad (1)$$

Where θ is shift angle with regard to antenna/beam boresight both is azimuth and elevation, θ_0 is the zero-power beamwidth, and G_0 is the maximum Gain. In Eq. (1), only the pattern among the main lobe is considered, and pattern in other angle ranges as the first and second sidelobe can also be modeled as the Sinc function. Design parameters are verified by comparison with field test results, as shown in Fig. 2. Once antenna pattern of a single beam is finished, one can get gains of both sum and difference channels by proper combination and the gains can be used to modulate target returns and abstract gimbal angle errors with regard to line-of-sight.

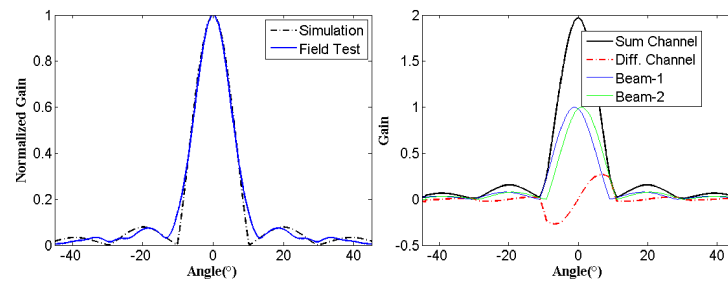


Fig. 2. Seeker antenna simulation results (left: pattern of single beam; right: gains of sum and difference channel).

2.3 Target scattering characteristics

An accurate target scattering model is taken into account by using the high frequency computation i.e. the physical optics method to compute target's far field scattering characteristics, especially the back scattering. The actual shape size of F-16 is chosen as a typical electrically large size target (about 70) to testify the effectiveness of physical optics approach. The non-uniform rational B-spline (NURBS) method is utilized for modeling and the mesh model is also established [8].

The frequency of the incident wave is 15.8 GHz; the wave incident elevation angle is 90° , and azimuth changes from 0° to 180° at a step of 10° . The scattering result in dBsm is shown in Fig. 3, in comparison with the Feko© result. It is shown that for the electrically large size complicated target the physical optics approach obtains high precision, and then it can be used in the PDRS modeling to reflect target's back scattering to generate target returns in seeker antenna aperture.

2.4 Receiver processing

As shown in Fig. 2, seeker receiver converts target returns to the intermediate frequency (IF) f_{IF} by the down-conversion.

Range gate τ_G is utilized to select target return while avoid outside clutter and noise. If filter and the AGC amplify signal to the certain level for consecutive narrow band filtering and I/Q demodulation. Different from conventional active radar seeker, the HPRF design utilizes the narrow band filtering to extract and track only the center spectrum line, in comparison to the matched filter. The quasi-continuous waveform is then obtained after narrow band filtering, and the following digital signal processor carries out target detection and tracking both in frequency domain. However, an assistant channel is also deployed to help observe a wider bandwidth, which provides an ECCM advantage and better clutter rejection, as in [5].

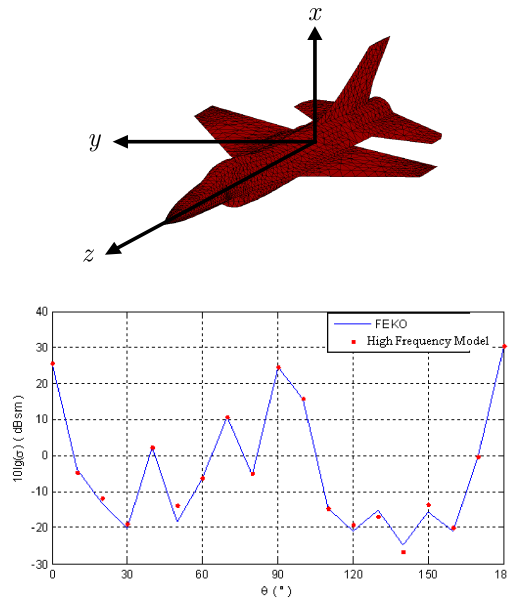


Fig. 3. Target scattering characteristics (left upper: plane target shape; right upper: mesh model; bottom: Feko and high frequency method comparison).

2.5 Digital signal processor

Functions of digital signal processor (DSP) include clutter cancellation, time domain weighting, FFT, frequency domain coherent/incoherent integration, CFAR, main controller and angle error measuring. DSP plays as a brain role in seeker to detect and track target in clutter, noise and may be ECM while change seeker state properly, as introduced in Fig. 4.

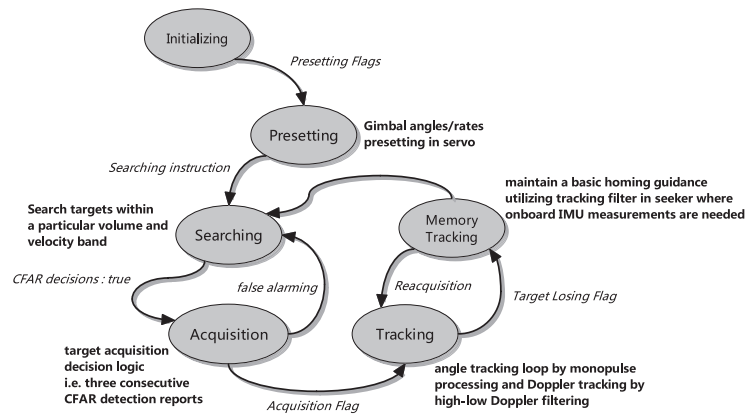


Fig. 4. Seeker status switching logic demonstration.

The HPRF design suffers from high range ambiguity and in seeker application we usually don't need a range track loop. So missile-to-target range won't be measured. Closing rate can be measured by tracking the center spectrum line in the bank of contiguous Doppler filters, which is usually referred to as the high-low Doppler filter. While the angle errors of line-of-sight with regard to antenna boresight, i.e. gimbal angle errors, can be measured by monopulse processing. The algorithms and models used in DSP can be found in [3, 6].

2.6 Tracking filter mechanism in data processing

As discussed in Section 2, an estimator in seeker has to be designed to help estimate LOS rates. To be more specific, the two rate components perpendicular to the LOS are needed and to provide estimates of these quantities is the basic task of a seeker system. In [7], a tracking filter for use with bearing-only measurement data is presented. The implementation is based on the Modified Spherical Coordinate (MSC) method. The MSC tracking filter utilizes a unique set of tracking states including two angles, two angle rates, inverse time-to-go range, as Eq. (2).

$$\mathbf{X} = [\varepsilon, \dot{\varepsilon}, \eta, \dot{\eta}, \rho, s]^T = [x_1, x_2, x_3, x_4, x_5, x_6]^T \quad (2)$$

where ε, η are the elevation and azimuth LOS angles and,

$$\omega = \dot{\eta} \cos \varepsilon, \quad \dot{\rho} = \frac{\dot{R}}{R}, \quad s = \frac{1}{R} \quad (3)$$

and the high non-linear equations of motion are defined by Eq. (4).

$$\dot{\mathbf{X}} = f(\mathbf{X}) = \begin{bmatrix} x_2 \\ -2x_2x_5 - x_4^2 \tan x_1 + x_6(a_{V_T} - a_{V_M}) \\ x_4/\cos x_1 \\ -2x_4x_5 + x_2x_4 \tan x_1 + x_6(a_{H_T} - a_{H_M}) \\ x_2^2 + x_4^2 - x_5^2 + x_6(a_{R_T} - a_{R_M}) \\ -x_5x_6 \end{bmatrix} \quad (4)$$

where $a_{V_T}, a_{H_T}, a_{R_T}$ are target accelerations in the vertical, horizontal and radical directions and $a_{V_M}, a_{H_M}, a_{R_M}$ are the corresponding SAM accelerations. The high non-linear feature of dynamic systems in Eq. (4) led to invalidation of the traditional Kalman filter. As a result, two extensions to it are considered. One can use the Extended Kalman filter (EKF), which is based on Taylor series approximation of the joint distribution, and the Unscented Kalman filter (UKF), which is respectively based on the unscented transformation of the joint distribution. To keep the implementation simple the continuous-time dynamic model in Eq. (4) was discretized using a simple Euler integration scheme. Note that this might be simple approach due to nonlinearities in the dynamics, so advanced integration scheme, such as Runge-Kutta might be more preferable.

3 Closed loop trajectory simulator

3.1 Guidance law

The basic guidance law is known as proportional navigation (PN). The intercept geometry is described in Fig. 5.

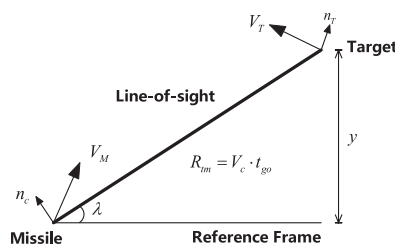


Fig. 5. The intercept geometry.

This guidance law can be written as Eq. (5).

$$n_c = N' V_c \dot{\lambda} \quad (5)$$

N' : effective navigation ratio.

V_c : closing velocity.

$\dot{\lambda}$: line-of-sight rate.

This expression can be rewritten as Eq. (6).

$$n_c = N' V_c \frac{d}{dt} \left(\frac{y}{V_c t_{go}} \right) = \frac{N'}{t_{go}^2} \underbrace{(y + \dot{y} t_{go})}_{ZEM} \quad (6)$$

t_{go} : time-to-go

y : altitude difference

\dot{y} : relative target rate

The term in the brackets represents the miss distance that would result (in the absence of target maneuver) if the SAM made no further corrective accelerations and is referred as the Zero Effort Miss (ZEM). PN will result in a zero miss distance if the target does not maneuver. While if the target maneuver (with acceleration n_T), then PN doesn't achieve anymore zero miss distance. In PN accelerations commands are proportional to the ZEM. Target maneuvers will modify the ZEM. Hence, an intuitive approach will be to include a corrective term in the ZEM to consider target maneuvers. The new guidance law is known as Augmented Proportional Navigation (APN), and can be written as Eq. (7).

$$n_c = \frac{N'}{t_{go}^2} \left(y + \dot{y} t_{go} + \frac{1}{2} n_T t_{go}^2 \right) \quad (7)$$

As we can see, the APN law needs an estimate of target acceleration to be able to compensate for target maneuvers. It also needs an estimate of time-to-go, which can be computed by seeker output.

3.2 Bank-to-turn control command

The control unit in SAM is designed to generate fin-angle instruction according to the APN accelerations commands. A bank-to-turn (BTT) control law is usually adopted as it can guide missile to the designated target while stabilize the body. Real-time missile flying status that includes the acceleration in both pitch and yaw axis and body rotation rates are needed. This control is somewhat complicated and can be found in [1].

Tail fins on missile body response to the above BTT control command to achieve actual fin angle in yaw, pitch and roll channel, respectively. The aerodynamic characteristic of SAM changes accordingly and so the missile flying status. Finally, we finish the 6-DOF closed loop trajectory simulation.

4 Case study

4.1 Scenario settings

A typical air defense operation scenario is designed. As we only focus on the terminal phase of engagement, the midcourse guidance utilizing inertial navigation solution isn't considered. Some key design parameters are listed in Table I.

Table I. Scenario settings

	Parameters	Values	Units and Notes
1.	initial target position, m	(7000, 1000, 0)	a reference frame, local level <i>North-Up-East</i> frame is used.
2.	initial target velocity, m/s	(200, 0, 0)	
3.	initial missile position, m	(0, 200, −400)	
4.	initial missile velocity, m/s	(600, 0, 0)	
5.	initial missile attitude	(0, 0, 0)	yaw, pitch and roll, °
6.	missile propulsion and mass	an experimental result for interpolation	
7.	aerodynamic coefficients	experimental rable for interpolation	
8.	effective navigation ratio	4	—
9.	trajectory update period	10	ms
Design parameters in pulsed Doppler radar seeker			
10.	seeker antenna characteristic	as illustrated in Fig. 3	
11.	target scattering features	as shown in Fig. 4	
12.	average transmitting power	350	W
13.	seeker carrier frequency	15.8	GHz
14.	intermediate frequency	30	MHz
15.	coherent pulse number	512	—
16.	pulse repetition frequency	320	Hz
17.	pulse width	2.0	μs
18.	gain loss overall	3.2	dB
19.	maximum detection range	35	km
20.	noise figure in receiver	6.8	dB
21.	seeker servo lag	0.05	1/s
22.	max antenna scanning rate	60	°/s
23.	seeker update period	40	ms

4.2 Results and analysis

The 6-DOF closed loop trajectory simulation is finished as follows. Real-time missile and target plane motion data is used in seeker receiver to generate target returns, in which involved the antenna model, target scattering, HPRF waveform induced eclipsing loss, missile-to-target radical induced Doppler shift and range induced wave propagation time delay. Target returns in both sum and difference channels are proceeded in receiver to convert to IF band. A narrow band filter is adopted to extract the central line in spectrum and convert the IF signals to the I/Q coherent video samples. Clutter cancellation and following Doppler filtering techniques help track this central line to form a closed target tracking in velocity. The monopulse method is used to measure gimbal angle errors. Those errors are sent to a tracking filter implemented in MSC. As soon as the estimations are obtained, one can adjust the range gate, Doppler tracking as well as angle tracking loop to finish a closed tracking. The inertial angular rate of LOS is estimated in above filter, and homing guidance is then accomplished by APN law. The fin-angle instruction is generated in BTT control unit to guide missile to target while stabilize missile body. Tail fins response the angle command; actual fin angles in three axes

is achieved. SAM is aerodynamically controlled, and a 6-DOF closed loop simulation is finally finished.

Firstly, missile-to-target relative motion in reference frame is shown in Fig. 6, where missile attitude is also described.

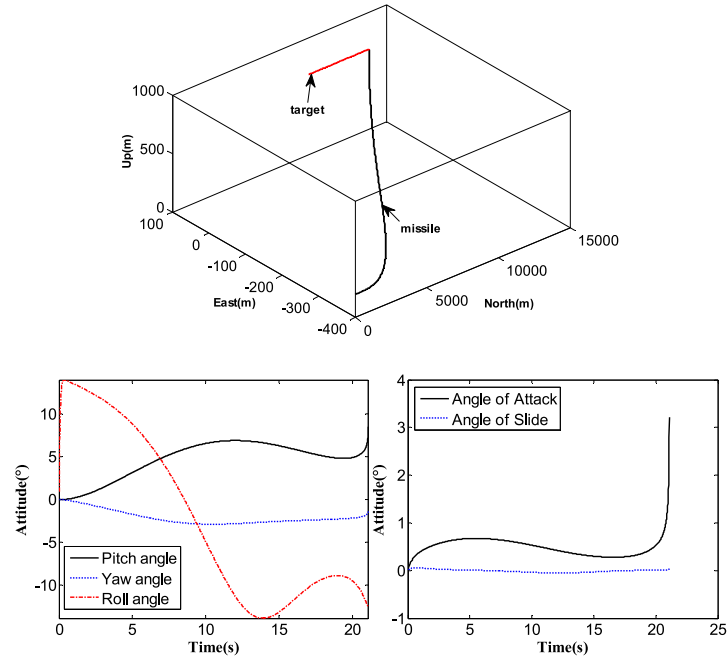


Fig. 6. Missile-to-target relative motion in reference frame.

Gimbal angle error measurements are shown in Fig. 7. By using monopulse processing techniques, one can extract those angle errors of target with regard to antenna boresight, i.e. gimbal. High measuring accuracy (approx. 1 mrad) is acquired, which provides an advantage of homing guidance precision and may be a better rejection of chaff and TRAD.

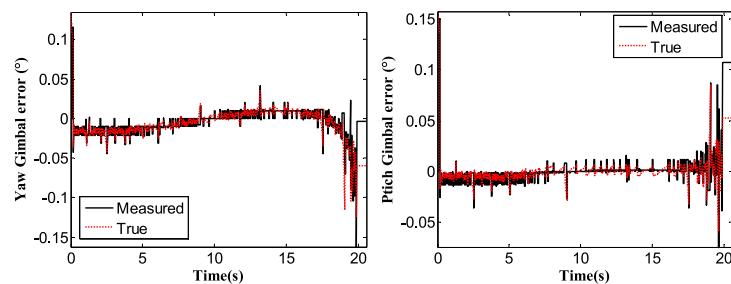


Fig. 7. Gimbal angle error measurements (left: yaw, right: pitch).

Gimbal angle error measurements are converted to LOS angles given current gimbal angles both in yaw and pitch axis.

4.3 ECM case

In ECM case e.g. velocity gate pull off (VGPO) jamming, the VGPO stopping period is 2.0 s, and VGPO period is 5.0 s, closed period is 3.0 s, the acceleration speed of VGPO is 20 m/s², the power ratio of jamming and target signal is 8.0, the

additional phase is $\pi/6$, time delay is $PW/2$, where PW is the pulse width of transmitted signal. Fig. 8 shows relative velocity measurement result within VGPO working period. It can be seen that a complete operation period is 8~10 s. However, in the short time interval of terminal guidance, about 20 s, it can only realize about 2 VGPO operation periods. As a result, the homing guidance precision is thus not affected much (the miss distance increases from 2.48 m to 8.0047 m). This illuminated the VGPO does affects the angular speed estimation astringency by guidance filtering, but it has no direct effect on the angle tracking loop with a relatively short time of terminal guidance, the typical value is 20 seconds. The conclusion was consistent with the anechoic chamber measurements results, which proved that the PDRS coherent video model provides an advantage of demonstrating the great impact made by the interferences on seeker homing accuracy and guidance precision.

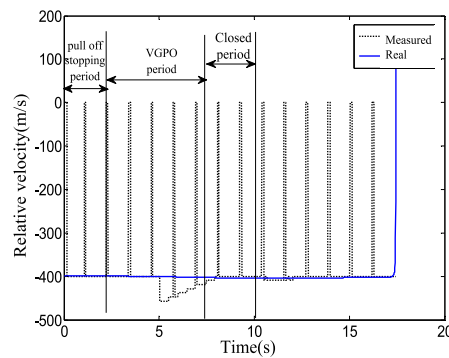


Fig. 8. Velocity measurement in VGPO case.

5 Conclusion

A coherent video model of PDRS for the 6-DOF closed loop trajectory simulation is discussed, and it offers an efficient tool to the design and evaluation of SAM. In an ECM case of VGPO jamming, simulation experiments are shown and the conclusion is consistent with anechoic chamber measurements results. The key point is that VGPO has no direct effect on the angle tracking loop, just through guidance filter to affects the angular speed estimation astringency. It achieves only 2 towing cycle within a relatively short time of terminal guidance. Results show that this PDRS coherent video model is accurate for 6-DOF trajectory simulation, and the closed loop simulation offers an effective and practical way to design parameters and evaluate performance of SAM.

Acknowledgments

This work is supported by the National Natural Science Foundation of China (No. 61301236).